CONCRETE LIBRARY OF JSCE NO. 29, JUNE 1997

STUDY ON PRACTICAL DESIGN METHOD FOR SHEAR OF REINFORCED CONCRETE SLABS LOADED NEAR FREE EDGE

(Translation from Proceedings of JSCE, No.532/V-30, February 1996)

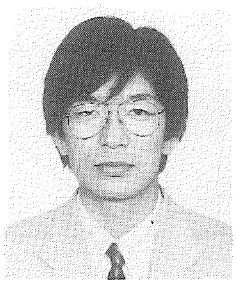
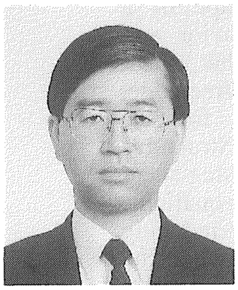


Hitoshi FURUUCHI   Yoshihiro TAKAHASHI   Yoshio KAKUTA

The punching shear capacity of reinforced concrete slabs decreases when a load is applied near the free edge. In the JSCE Standard Specification for Design and Construction of Concrete Structures, loss in capacity is taken into account by shortening the peripheral length of the cross section designed to resist punching shear. On the basis of experiments on simply supported slabs with a free edge this study reveals that the JSCE method does not adequately take into account the effect of the free edge. A new method of evaluating the ultimate shear capacity in such cases is discussed and two practical design methods are proposed; one entailing shortening the peripheral length of the design cross section while at the same time reducing the punching shear capacity per unit length of the design cross section, and the other assuming a slab as the beam with an effective width and applying the beam shear equation to the slab.

Key Words: *reinforced concrete slabs, punching shear, free edges, critical section, beam shear, design*

Hitoshi Furuuchi is a Research Associate in the Department of Civil Engineering at Hokkaido University, Sapporo, Japan. His research interests relate to the dowel action of reinforcing bars and the mechanism of diagonal tension failure in reinforced concrete members. He is a member of the JSCE.

Yoshihiro Takahashi is a Professor in the Department of Civil Engineering at Hokkai Gakuen University, Sapporo, Japan. He obtained his D.Eng. from Hokkaido University in 1982. His research interests relate to the shear capacity of reinforced concrete members. He is a member of the JSCE.

Yoshio Kakuta is a Professor in the Department of Civil Engineering at Hokkaido University, Sapporo, Japan. He obtained his D.Eng. from Hokkaido University in 1968. His research interests include cracking deflection, the shear strength and fatigue of reinforced concrete members, partially prestressed concrete, and the application of continuous fiber reinforcing materials to concrete structures. He is a member of the JSCE.

1. INTRODUCTION

In RC slabs subjected to concentrated loading and in RC footings that directly support a load transferred from a column, there is a possibility of punching shear failure, a failure similar to beam shear failure or flexural failure due to the development of yielding lines. Punching shear failure is a particular brittle failure in which the loaded concrete falls out in the shape of a pyramid. It is known that this behavior and resistance to it is complex, and that shear capacity falls as the load approaches a free edge. The JSCE's Standard Specification for the Design and Construction of Concrete Structures [1] gives design equations for the punching shear capacity of planar members. In these equations, punching shear capacity is ensured by reducing the length of the design cross section when the loading point is near the free edge of a slab. However, it was been pointed out that this method does not adequately take into account the effect of the free edge on shear punching [2].

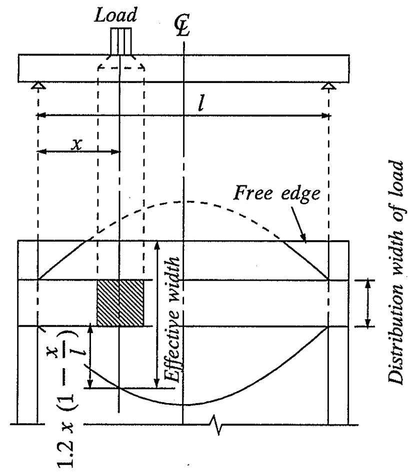

Fig. 1 Effective width of one- way slab

In this study, the JSCE method is re-evaluated based on experimental results of punching shear on one-way RC slabs with the purpose of proposing a new and practical design method for such cases.

2. JSCE DESIGN METHOD FOR SLABS

2.1 Design Flexural Capacity of Planar Members

In the JSCE Standard Specification, the bending moment of a planar member is in principle evaluated by linear analysis, but the use of plastic analysis by the theory of yield lines or the strip method is also permitted. Simply supported one-way slabs subjected to a concentrated load can be designed as beam with an effective width, as shown in Fig.1. This method is based on a bending moment distribution given by elastic theory. The effective width b_e may be computed from Eqs.(1) and (2).

$$\text{when} \quad c \geq 1.2x(1 - x/l), \qquad b_e = v + 2.4x(1 - x/l) \tag{1}$$

$$c < 1.2x(1 - x/l), \qquad b_e = c + v + 1.2x(1 - x/l) \tag{2}$$

where c : distance from edge of distributed load to the free edge of slab

x : distance from the center of distributed load to nearest support of the slab

l : span of slab

v : width of distributed load

2.2 Design Shear Capacity of Planar Members

For a planar member subjected to transverse shear, the examination of shear as a linear member and the examination of punching shear should be made according to the JSCE Standard Specification. However, a method of taking a definite effective width as a linear member is not given for planar member. For the examination of punching shear, the provision below is provided.

2.3 Design punching shear capacity of planar members

When a concentrated load is applied to a localized area of a planar member such as an RC slab, the design punching shear capacity is determined by Eq.(3).

$$V_{pcd} = \beta_d \, \beta_p \, \beta_r \, f_{pcd} \, u_p \, d \, / \, \gamma_b \qquad (3)$$

where, $f_{pcd} = 0.19\sqrt{f'_{cd}}$ (MPa) (4)

$\beta_d = \sqrt[4]{100/d}$ $(d{:}cm)$ when $\beta_d > 1.5$, β_d is taken as 1.5

$\beta_p = \sqrt[3]{100p}$ when $\beta_p > 1.5$, β_p is taken as 1.5

$\beta_r = 1 + 1/(1 + 0.25\,u/d)$

f'_{cd} : design compressive strength of concrete (MPa)

u : peripheral length of loaded area

u_p : peripheral length of the design cross section at a point $d/2$ from the loaded area

d, p : effective depth and reinforcement ratio defined as average values of reinforcement in the two directions

γ_b : member factor (1.3 in general)

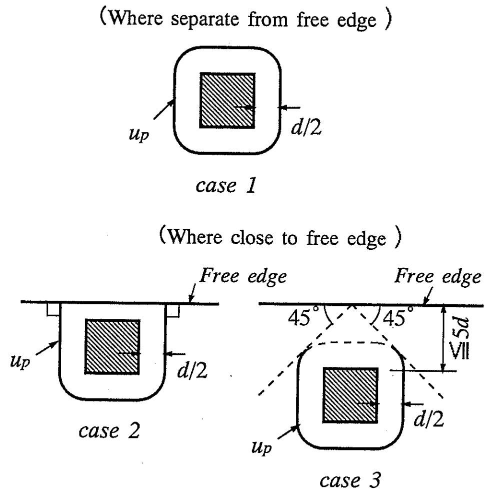

Fig. 2 Design cross section

Equation (3) was derived by the modifying the equation for the shear capacity of beams to make it suitable for punching shear according to experimental results on RC slabs [3] and footings [4]. The average ratio of experimental to calculated values of punching shear capacity is 1.033 and the ratio of the standard deviation to the average is 0.159 [5].

When the load acts in the vicinity of a free edge or opening in the member, it is according for by reducing the peripheral length of the design cross section u_p, thus reducing the punching shear capacity. The method of this reduction in u_p is determined as given in the CEB/FIP Model Code 1978 [6], in which the value of u_p is taken as the smallest value of cases 1 to 3 as shown in Fig.2.

In the CEB/FIP Model Code 1990 [7], case 3 is removed and the location of the design cross section is modified to be 2d from the loaded area. Then the peripheral length of the design cross section is taken as the shorter of cases 1 and 2.

In other countries, the location of the design cross section is set as d/2 and 1.5d from the loaded area in the ACI318 building code [8] and the Euro-code [9], respectively.

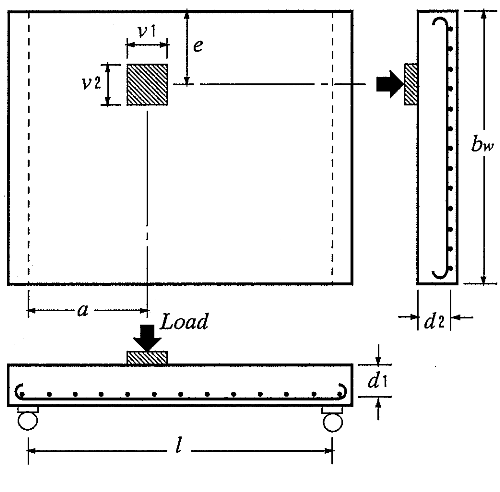

Fig.3 Specimen

3. OUTLINE OF PUNCHING SHEAR EXPERIMENTS

An outline of experimental results used in this study follows. The specimens were reinforced concrete slabs simply supported on two opposite sides, as shown in Fig.3. The main test parameters were the size of the slabs (width, span, and thickness) and loading conditions (location and distribution area) as shown in Table.1. This table also shows the compressive strength of the concrete, the yield strength of the reinforcing bars, and the ultimate load on the specimens. Concrete strength ranged from 21.8 to 37.3 MPa. The reinforcing bars were hot-rolled deformed bars with a nominal yield point of 345 MPa and diameters of 10 and 13 mm. The ends of longitudinal bars are anchored by hooks and the transverse bars are anchored by connect on to the outermost longitudinal bars. The specimens were supported by round steel bars held between steel plates of thickness 1cm and width 10cm, and the four corners of the specimens were free to rise. Steel plates of thickness of 3 cm were used as loading pads on the specimens.

The failure modes are shown in Table 1; these were determined by observation after the specimens failed. Punching shear failure, a shear failure similar to beam shear failure, a combination of these failure modes, and flexural failure due to developed yield lines were observed, as shown in Fig .4. For the combined type of shear failure, a punched concrete section of pyramid shape was partially removed at the free edge and diagonal cracks were observed on the side of the slab. The shear failure similar to beam shear failure was observed in slabs of comparatively small width. In case of the slabs with small shear span, it seems that the failure mode was a shear-compression failure as observed in deep beams.

Table 1 Details of Specimens and Experimental Results

No.	Specimen Name	Span l (cm)	Width b_w (cm)	Hight h (cm)	Effective Depth d_1 (cm)	d_2 (cm)	Loaded Area v_1 (cm)	v_2 (cm)	1) a (cm)	2) e (cm)	Reinforcement Ratio p_1 (%)	p_2 (%)	3) f_y (MPa)	4) f_c' (MPa)	5) P_B (kN)	Failure * Mode
1	H56-05	50.0	30.0	10.0	8.0	7.0	10.0	10.0	25.0	15.0	1.67	1.91	400	31.0	108	BM
2	H56-06	50.0	30.0	10.0	8.0	7.0	10.0	10.0	25.0	10.0	1.67	1.91	400	29.3	98	BM
3	H56-07	50.0	50.0	10.0	8.0	7.0	10.0	10.0	25.0	25.0	1.67	1.91	400	29.9	168	PS
4	H56-08	50.0	50.0	10.0	8.0	7.0	10.0	10.0	25.0	17.5	1.67	1.91	400	29.9	141	PS
5	H56-09	50.0	50.0	10.0	8.0	7.0	10.0	10.0	25.0	10.0	1.67	1.91	400	30.3	102	PS
6	H56-10	50.0	70.0	10.0	8.0	7.0	10.0	10.0	25.0	35.0	1.67	1.91	400	33.0	183	PS
7	H56-11	50.0	70.0	10.0	8.0	7.0	10.0	10.0	25.0	22.5	1.67	1.91	400	33.0	152	PS
8	H56-12	50.0	70.0	10.0	8.0	7.0	10.0	10.0	25.0	10.0	1.67	1.91	400	33.0	110	PS
9	H56-13	50.0	100.0	10.0	8.0	7.0	10.0	10.0	25.0	50.0	1.67	1.91	400	31.7	199	PS
10	H56-14	50.0	100.0	10.0	8.0	7.0	10.0	10.0	25.0	40.0	1.67	1.91	400	28.6	174	PS
11	H56-15	50.0	100.0	10.0	8.0	7.0	10.0	10.0	25.0	30.0	1.67	1.91	400	26.9	180	PS
12	H56-16	50.0	100.0	10.0	8.0	7.0	10.0	10.0	25.0	20.0	1.67	1.91	400	28.2	160	PS
13	H56-17	50.0	100.0	10.0	8.0	7.0	10.0	10.0	25.0	10.0	1.67	1.91	400	31.1	129	PS
14	H56-18	100.0	50.0	10.0	8.0	7.0	10.0	10.0	50.0	25.0	1.67	1.91	400	31.0	85	BM
15	H56-19	100.0	50.0	10.0	8.0	7.0	10.0	10.0	50.0	10.0	1.67	1.91	400	28.4	82	PS
16	H56-20	100.0	70.0	10.0	8.0	7.0	10.0	10.0	50.0	35.0	1.67	1.91	400	30.1	124	BM
17	H56-21	100.0	70.0	10.0	8.0	7.0	10.0	10.0	50.0	10.0	1.67	1.91	400	37.3	93	PS
18	H56-22	100.0	100.0	10.0	8.0	7.0	10.0	10.0	50.0	50.0	1.67	1.91	400	32.0	175	PS
19	H56-23	100.0	100.0	10.0	8.0	7.0	10.0	10.0	50.0	10.0	1.67	1.91	400	27.2	88	PS
20	H56-24	100.0	140.0	10.0	8.0	7.0	10.0	10.0	50.0	70.0	1.67	1.91	400	34.5	214	PS
21	H56-25	100.0	140.0	10.0	8.0	7.0	10.0	10.0	50.0	55.0	1.67	1.91	400	30.4	184	PS
22	H56-26	100.0	140.0	10.0	8.0	7.0	10.0	10.0	50.0	40.0	1.67	1.91	400	29.0	174	PS
23	H56-27	100.0	140.0	10.0	8.0	7.0	10.0	10.0	50.0	25.0	1.67	1.91	400	31.5	140	PS
24	H56-28	100.0	140.0	10.0	8.0	7.0	10.0	10.0	50.0	10.0	1.67	1.91	400	27.2	96	PS
25	H56-29	100.0	140.0	20.0	18.0	17.0	10.0	10.0	50.0	40.0	1.13	1.20	400	36.5	431	PS
26	H56-30	100.0	140.0	20.0	18.0	17.0	10.0	10.0	50.0	25.0	1.13	1.20	400	31.6	349	PS
27	H56-31	100.0	140.0	20.0	18.0	17.0	10.0	10.0	50.0	10.0	1.13	1.20	400	29.7	196	PS
28	H57-61	100.0	140.0	20.0	18.0	17.0	10.0	10.0	50.0	70.0	1.10	1.16	399	30.1	470	PS
29	H57-62	100.0	140.0	20.0	18.0	17.0	10.0	10.0	50.0	60.0	1.10	1.16	399	31.5	503	PS
30	H57-63	100.0	140.0	20.0	18.0	17.0	10.0	10.0	50.0	45.0	1.10	1.16	399	30.7	444	PS
31	H57-64	100.0	140.0	20.0	18.0	17.0	10.0	10.0	50.0	30.0	1.10	1.16	399	30.1	372	PS

32	H57-65	100.0	140.0	20.0	18.0	17.0	10.0	10.0	50.0	15.0	1.10	1.16	399	30.5	270	PS
33	H57-66	100.0	120.0	20.0	18.0	17.0	10.0	10.0	50.0	60.0	1.10	1.16	399	33.5	478	PS
34	H57-67	100.0	120.0	20.0	18.0	17.0	10.0	10.0	50.0	45.0	1.10	1.16	399	34.8	458	PS
35	H57-68	100.0	120.0	20.0	18.0	17.0	10.0	10.0	50.0	30.0	1.10	1.16	399	35.9	418	PB
36	H57-69	100.0	120.0	20.0	18.0	17.0	10.0	10.0	50.0	15.0	1.10	1.16	399	32.3	255	PB
37	H57-70	100.0	90.0	20.0	18.0	17.0	10.0	10.0	50.0	45.0	1.10	1.16	399	30.1	405	PS
38	H57-71	100.0	90.0	20.0	18.0	17.0	10.0	10.0	50.0	30.0	1.10	1.16	399	31.9	378	PB
39	H57-72	100.0	90.0	20.0	18.0	17.0	10.0	10.0	50.0	15.0	1.10	1.16	399	34.9	296	PB
40	H57-73	100.0	60.0	20.0	18.0	17.0	10.0	10.0	50.0	30.0	1.10	1.16	399	28.0	282	BS
41	H57-74	100.0	60.0	20.0	18.0	17.0	10.0	10.0	50.0	15.0	1.10	1.16	399	35.1	157	BS
42	H57-75	100.0	30.0	20.0	18.0	17.0	10.0	10.0	50.0	15.0	1.10	1.16	399	31.5	160	BS
43	G57-41	100.0	140.0	10.0	8.0	7.0	7.0	14.0	50.0	70.0	1.70	1.94	419	31.2	190	PS
44	G57-42	100.0	140.0	10.0	8.0	7.0	7.0	14.0	50.0	55.0	1.70	1.94	419	33.7	164	PS
45	G57-43	100.0	140.0	10.0	8.0	7.0	7.0	14.0	50.0	40.0	1.70	1.94	419	33.4	180	PS
46	G57-44	100.0	140.0	10.0	8.0	7.0	7.0	14.0	50.0	25.0	1.70	1.94	419	28.4	138	PS
47	G57-45	100.0	140.0	10.0	8.0	7.0	7.0	14.0	50.0	10.0	1.70	1.94	419	32.6	102	PS
48	G57-46	100.0	140.0	10.0	8.0	7.0	14.0	7.0	50.0	70.0	1.70	1.94	419	31.6	188	PS
49	G57-47	100.0	140.0	10.0	8.0	7.0	14.0	7.0	50.0	55.0	1.70	1.94	419	26.6	165	PS
50	G57-48	100.0	140.0	10.0	8.0	7.0	14.0	7.0	50.0	40.0	1.70	1.94	419	27.7	154	PS
51	G57-49	100.0	140.0	10.0	8.0	7.0	14.0	7.0	50.0	25.0	1.70	1.94	419	24.4	149	PS
52	G57-50	100.0	140.0	10.0	8.0	7.0	14.0	7.0	50.0	10.0	1.70	1.94	419	27.1	89	PS
53	G57-81	100.0	140.0	10.0	8.0	7.0	10.0	10.0	65.0	70.0	1.70	1.94	419	24.2	157	PS
54	G57-82	100.0	140.0	10.0	8.0	7.0	10.0	10.0	65.0	55.0	1.70	1.94	419	28.7	147	PS
55	G57-83	100.0	140.0	10.0	8.0	7.0	10.0	10.0	65.0	40.0	1.70	1.94	419	26.7	152	PS
56	G57-84	100.0	140.0	10.0	8.0	7.0	10.0	10.0	65.0	25.0	1.70	1.94	419	27.0	123	PS
57	G57-85	100.0	140.0	10.0	8.0	7.0	10.0	10.0	65.0	10.0	1.70	1.94	419	26.9	82	PS
58	G58-01	100.0	140.0	10.0	8.0	7.0	7.5	7.5	50.0	70.0	1.67	1.91	412	32.0	154	PS
59	G58-02	100.0	140.0	10.0	8.0	7.0	7.5	7.5	50.0	55.0	1.67	1.91	412	33.1	134	PS
60	G58-03	100.0	140.0	10.0	8.0	7.0	7.5	7.5	50.0	40.0	1.67	1.91	412	30.7	144	PS
61	G58-04	100.0	140.0	10.0	8.0	7.0	7.5	7.5	50.0	25.0	1.67	1.91	412	35.5	135	PS
62	G58-05	100.0	140.0	10.0	8.0	7.0	7.5	7.5	50.0	10.0	1.67	1.91	412	30.5	85	PS
63	G58-06	100.0	140.0	10.0	8.0	7.0	15.0	15.0	50.0	70.0	1.67	1.91	412	31.2	179	PS
64	G58-07	100.0	140.0	10.0	8.0	7.0	15.0	15.0	50.0	55.0	1.67	1.91	412	32.2	186	PS
65	G58-08	100.0	140.0	10.0	8.0	7.0	15.0	15.0	50.0	40.0	1.67	1.91	412	30.8	187	PS
66	G58-09	100.0	140.0	10.0	8.0	7.0	15.0	15.0	50.0	25.0	1.67	1.91	412	36.0	157	PS
67	G58-10	100.0	140.0	10.0	8.0	7.0	15.0	15.0	50.0	10.0	1.67	1.91	412	31.2	96	PS
68	G58-11	100.0	140.0	15.0	13.0	12.0	10.0	10.0	50.0	70.0	1.03	1.12	412	31.7	306	PS
69	G58-12	100.0	140.0	15.0	13.0	12.0	10.0	10.0	50.0	55.0	1.03	1.12	412	32.7	294	PS
70	G58-13	100.0	140.0	15.0	13.0	12.0	10.0	10.0	50.0	40.0	1.03	1.12	412	34.2	281	PS
71	G58-14	100.0	140.0	15.0	13.0	12.0	10.0	10.0	50.0	25.0	1.03	1.12	412	32.8	223	PS
72	G58-15	100.0	140.0	15.0	13.0	12.0	10.0	10.0	50.0	20.0	1.03	1.12	412	32.7	187	PS
73	G58-16	100.0	140.0	15.0	13.0	12.0	10.0	10.0	50.0	10.0	1.03	1.12	412	30.9	143	PS
74	G58-17	100.0	140.0	15.0	12.9	11.7	10.0	10.0	50.0	70.0	1.84	1.00	430	36.3	312	PS
75	G58-18	100.0	140.0	15.0	12.9	11.7	10.0	10.0	50.0	55.0	1.84	1.00	430	33.6	306	PS
76	G58-19	100.0	140.0	15.0	12.9	11.7	10.0	10.0	50.0	40.0	1.84	1.00	430	28.2	278	PS
77	G58-20	100.0	140.0	15.0	12.9	11.7	10.0	10.0	50.0	25.0	1.84	1.00	430	31.7	236	PS
78	G58-21	100.0	140.0	15.0	12.9	11.7	10.0	10.0	50.0	10.0	1.84	1.00	430	30.8	152	PS
79	G60-04	70.0	90.0	15.0	12.9	11.6	10.0	10.0	35.0	45.0	1.55	1.72	402	29.2	302	PS
80	G60-07	70.0	90.0	15.0	12.9	11.6	10.0	10.0	35.0	30.0	1.55	1.72	402	29.5	335	PS
81	G60-10	70.0	90.0	15.0	12.9	11.6	10.0	10.0	35.0	30.0	1.55	1.72	402	21.8	258	PS
82	G60-13	70.0	90.0	15.0	12.9	11.6	10.0	10.0	35.0	6.0	1.55	1.72	402	28.0	103	PS
83	G60-16	70.0	15.0	15.0	12.9	11.6	10.0	10.0	35.0	7.5	1.55	1.72	402	23.6	50	BS
84	G60-19	70.0	30.0	15.0	12.9	11.6	10.0	10.0	35.0	15.0	1.55	1.72	402	23.6	109	BS
85	G60-22	70.0	45.0	15.0	12.9	11.6	10.0	10.0	35.0	22.5	1.55	1.72	402	28.5	162	BS
86	G60-25	70.0	60.0	15.0	12.9	11.6	10.0	10.0	35.0	30.0	1.55	1.72	402	28.5	230	PB

1) Shear span
2) Distance from Free edge to Loading Point
3) Yielding Point of Longitudinal Bar
4) Compressive Stregth of Concrete
5) Ultimate Load

* BM : Flexural Failure
PS : Punching Shear Failure
BS : Shear Failure similar to Beam Shear Failure
PB : Combination of Punching Shear and Beam Shear Failure

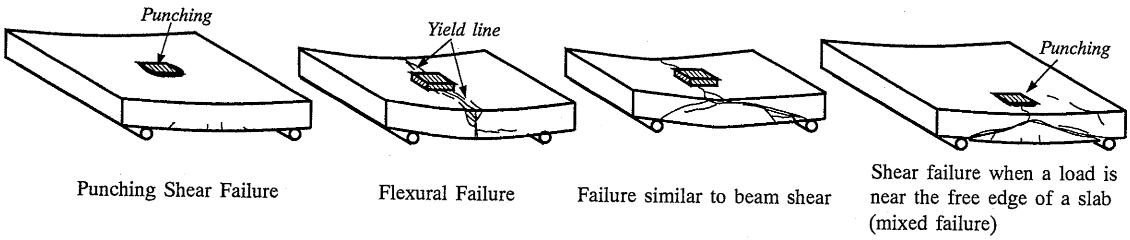

Fig. 4 Failure mode

4. DISCUSSION OF ULITIMATE CAPACITY OF RC SLABS

4.1 Evaluation of Flexural Capacity of RC Slabs

Four of a total of 86 slabs failed as a result of longitudinal bar yielding and the development of yield lines. The flexural capacity of the slabs increased somewhat with large deformation after yielding of the longitudinal bars. In these slabs, the flexural capacity was attributable to the full width of the slabs, because the yield lines developed over the full width on the center line of the slabs, including the loading point. The capacity of the slabs was computed for a point load, as the effect of the loading area is negligibly small. The results are as follows.

H56-05 89.57 kN (1.21)
H56-06 88.89 kN (1.10)
H56-18 74.67 kN (1.14)
H56-20 104.1 kN (1.19)

The flexural capacity of specimen H56-20 is nearly equal to the punching shear capacity, but in other specimens the flexural capacity is smaller than the punching shear capacity. The values shown in parenthesis are the ratio of experimental to calculated values of flexural capacity. The calculated values are on the safe side as compared with the test results. In general, it is known that the actual ultimate flexural capacity is greater than that obtained from the mechanism of yield lines. Thus it can be said that results given above are appropriate.

4.2 Punching Shear Capacity of Slabs Loaded Near Free Edge

It is known that punching shear capacity decreases as an applied load approaches a free edge [2]. Figure 5 shows the relationship between loading position and shear capacity. The lateral axis is e/a, a parameter representing the loading position in which a is the shear span and e is the distance from the free edge to the loading point. This figure plots the experimental shear capacities multiplied by $\sqrt{30 / f_c'}$ to eliminate deviations in concrete strength from 30 MPa. The solid line in this figure is computed using Eq.(3) with the member factor γ_b set to 1.0 so as to investigate agreement with the test results. Cases 1 to 3 show the shortest design cross section for each e/a. It can be seen from this figure that the experimental shear capacity gradually falls as the value of e/a becomes

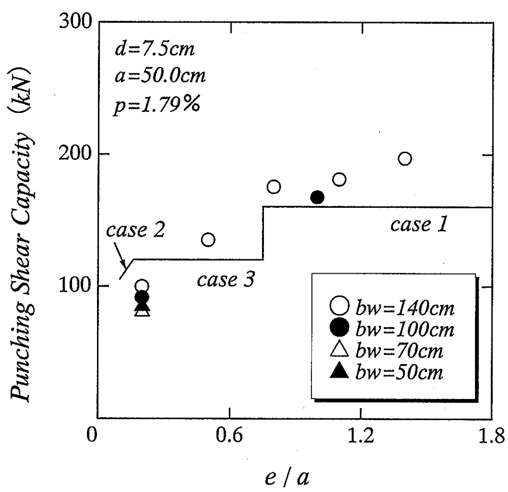

Fig.5 Effect of free edge on the punching shear capacity

smaller. The design cross section transfers from case 1 to case 3 when the distance from the end of the load distribution to the free edge becomes smaller than five times of the effective depth, according to the JSCE Standard Specification. Therefore, the evaluated punching shear capacity changes discontinuously and gives safer values for loading points not so close to the free edge. On the other hand, when the loading point is located very close to the free edge, the evaluated capacity is smaller than the actual capacity in spite of the case 2 design cross section being used. It can thus be said that the experimental values of punching shear differ from the ones evaluated when the effect of the free edge is taken into account only by reducing the peripheral length of the design cross section, and that a failure mode with a critical section such as case 3 could not be observed in the experiments.

It would appear satisfactory, therefore, either case 1 or case 2 as the peripheral length of the design cross section. Furthermore it may be concluded that shear strength per unit length of the design cross section f_{pcd} decreases due to the effect of free edges. Here the punching shear capacity is assumed to be given by the following equations with a strength reduction coefficient α.

$$\text{Shear Capacity} = \beta_d \beta_p \beta_r f_p u_p d \qquad (5)$$

where, $f_p = \alpha \times 0.19\sqrt{f_c'}$ (MPa)

f_c': Concrete compressive strength from the tests (MPa)

α: Coefficient representing the decrease in shear strength per unit length of the design cross section

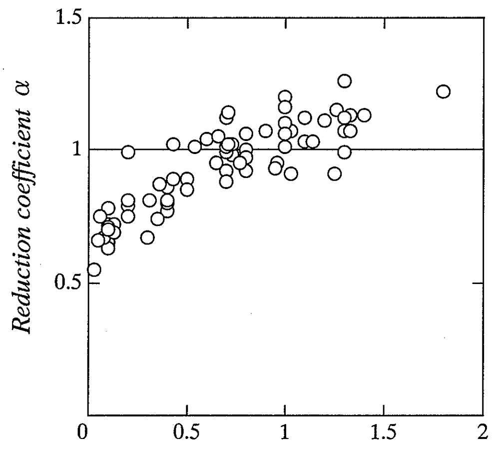

Fig.6 Decrease in shear strength per unit length of the design cross section

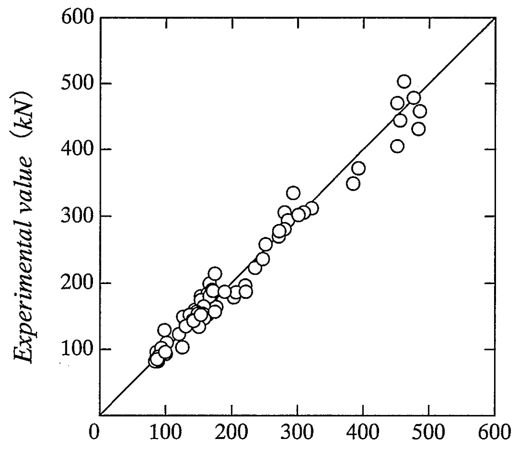

Fig.7 Punching shear capacity

Figure 6 shows the relation between α and e'/a, in which e' is the distance from the edge of the loading area to the free edge, $e - v_2/2$. The test results for all specimens that failed by punching shear are plotted in this figure. The shear strength decreases gradually as e'/a becomes smaller and the slabs have an ordinary punching shear capacity when the load is sufficiently far from a free edge. However, they have a reduced shear strength when the load is close to a free edge. Furthermore, when the load is very close to a free edge, the capacity decreases more rapidly due to the effect of the reduction in peripheral length of the design cross section as well as the decrease in shear strength per unit length of the design cross section. As other parameter, e'/h and others were examined; however these parameters appear to have almost no effect on the shear strength. The following equation for α was obtained by linear regression analysis:

$$\alpha = 0.64 + 0.46\, e'/a \qquad (6)$$

when $\alpha > 1.0$, α is taken as 1.0

where, e' : distance from an end of loaded area to a free edge

The relationship between experimental results and calculations when reduction coefficient α is applied to punching shear capacity is shown in Fig.7. The average value of the ratio of experimental to calculated values of shear capacity is 1.01 and the coefficient of variation is 9.1% for the 71 slabs.

4.3 Evaluation by Shear Capacity as a Beam

The reduction coefficient α derived in the preceding section can be used only for simply supported one-way slabs, so values of α must be investigated experimentally for slabs with other supporting conditions. Here, a method of evaluation based on beam shear capacity in place of the method mentioned above. A wide slab fails by complete punching shear failure, but a slab with a smaller width fails in the beam shear mode. In the preceding section, an intermediate type of failure between punching shear failure and beam shear failure is treated as an imperfect punching failure. Such a failure might also be considered an imperfect beam shear failure in which the full member width is not effective. Thus, if the slab is considered as a beam adopting an effective is an important problem. In the JSCE Standard Specification, the effective width is given for flexural capacity but not explicitly stated for shear failure. In this study, the effective width used in determining the shear capacity of a slab is assumed to be the same as for flexural capacity, as shown Fig.1. Equations (7) and (8) are used to evaluate shear capacities. These equations are for ordinary beams and deep beams, respectively, which are the basis of the JSCE equations.

$$V_c = 0.20\,(p_w f_c')^{1/3} d^{-1/4} (0.75 + \frac{1.4}{a/d})\, b_w d \qquad (7)$$

where, b_w : width of member

d : effective depth (m)

$p_w = 100 \cdot A_s / (b_w d)$

A_s : area of tensile reinforcement

f_c' : compressive strength of concrete

The above equation is for a diagonal tension failure of RC beams without web reinforcement and was derived through reevaluation of the effect of reinforcement ratio and the size effect by J. Niwa et al [10].

$$V_{wd} = \frac{0.24\, f_c'^{2/3} (1 + \sqrt{p_w})(1 + 3.33\, r/d)}{1 + (a/d)^2} b_w d \qquad (8)$$

where, r : width of plate at support

This equation is for the compression shear failure of deep beams based on a tied arch model proposed by J. Niwa [11].

The shear capacity of the RC slab as a beam is found by selecting the larger value of V_c and V_{wd}. Generally, specimens used in the study of beam shear capacity are loaded symmetrically at two points . However, the RC slabs used in this study were loaded at one point and different widths of support and loading plates were used. It is assumed that the shear span used to compute the shear capacity of deep beams is as shown in Fig.8. On this assumption, it can be shown that the shear capacity increases as the loaded plate is made wider. However, this is a provisional assumption and it is necessary to reconsider how to modify the tied arch mechanism to account for the size of the loaded plate.

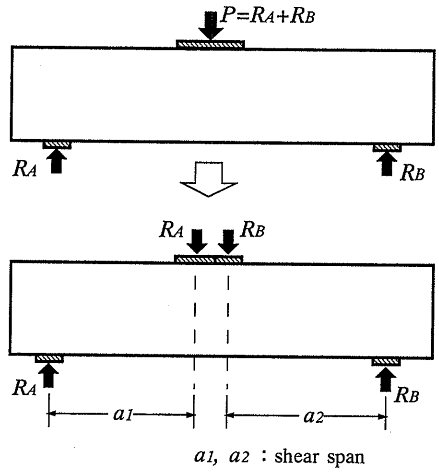

Fig. 8 Definition of shear span

Those slabs in which the shear strength decreased due to effect of the free edge ($e'/a \leq 0.78$) are considered in the following discussion. Figures 9.1 and 9.2 show the results for which the beam shear capacity obtained by Eqs.(7) and (8) is smaller than the punching shear capacity, respectively. In these figures, the punching shear capacities in which the reduction coefficient α is not used are plotted with crosses for reference. These results demonstrate that beam shear capacity calculated using the effective width agrees well with the experimental results in comparison with the punching shear capacity. It seems that the shear capacity can be ensured by assuming a slab as the beam with an effective width when a load locates near the free edge.

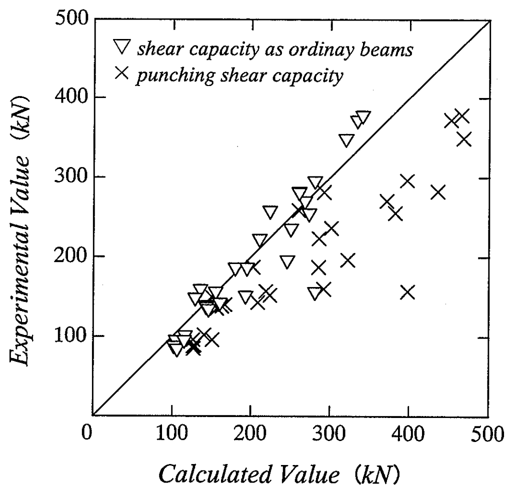

Fig.9.1 Shear Capacity as ordinary beams

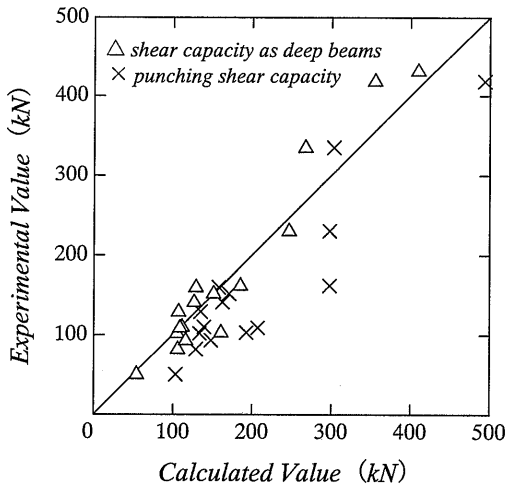

Fig.9.2 Shear Capacity as Deep Beams

4.4 Proposal for Method of Evaluating Ultimate Capacity of RC Slabs

From the results described above, the following methods of evaluating the ultimate capacity of RC slabs can be proposed:

For the failure due to bending moment:
1) Ultimate flexural capacity computed by yield line theory

For the shear failure:
2) Complete punching shear capacity using case 1 design cross section without considering the effect of free edges
3) Punching shear capacity using case 1 or case 2 design cross section taking into account the effect of free edges as a reduction coefficient
4) Beam shear capacity using the effective width as with flexural capacity, adapting the larger of the capacities calculated by the equations for ordinary beams and for deep beams.

In method A, the smallest of 1), 2), and 3) is selected as the ultimate capacity of the RC slab. In method B, the smallest of 1), 2), and 4) is selected. For all specimens, the results evaluated by methods A and B are shown in Figs. 10.1 and 10.2. The average ratios of experimental shear capacities to values calculated by methods A and B are 1.01 and 1.03, and the coefficients of variation are 8.5 % and 14.0 %, respectively. This demonstrates the validity of the evaluation of RC slab shear capacity of by each method. The effective width of a slab used in method B is based on elastic analysis and therefore has the advantage of being easily expand able to arbitrary support conditions. Consequently, method B is recommended as a practical method for evaluating capacity.

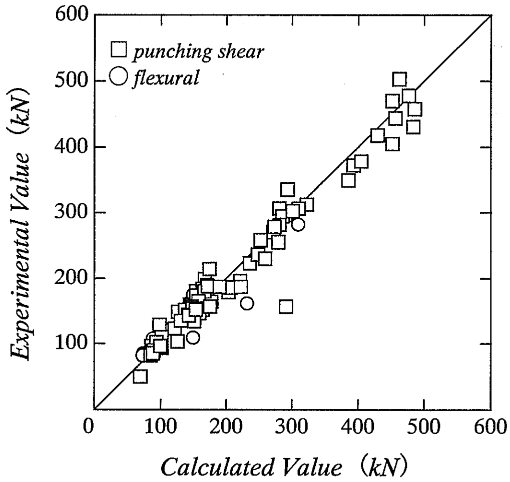

Fig.10.1 Capacity of Slabs (Method A)

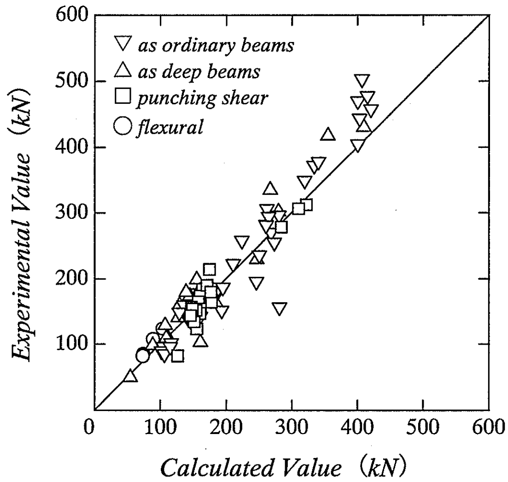

Fig.10.2 Capacity of Slabs (Method B)

5. CONCLUSION

The following conclusions result from this discussion of the shear capacity of one-way RC slabs subjected to loading near a free edge.

1) It is found from experimental results that the shear capacity of RC slabs falls as the load approaches a free edge.

2) The punching shear capacity calculated by reducing the peripheral length of the design cross section when the load is near the free edge according to the JSCE Standard Specification is smaller than the test result when the load is very close to the free edge.

3) The shear capacity calculated using the design cross section of case 3 as shown in Fig.2, which is applied when the distance from the edge of the loading area to the free edge is less than five times the effective depth, does not agree with the experimental results either quantitatively or qualitatively.

4) By removing the design cross section of case 3 from the JSCE Standard Specification and by introducing a reduction coefficient to account for the effect of loading close to a free edge, the punching shear capacity of the slabs can be evaluated satisfactorily.

5) As another method of evaluating the shear capacity of a slab loaded near a free edge, the JSCE design equations for an ordinary beam or a deep beam are applicable with a good accuracy by taking an effective width of a slab same as the one taking in the flexural design.

6) A practical design method is proposed in which the capacity of RC slabs is determined as the smallest v
alue of flexural capacity, beam shear capacity with an effective width, and punching shear capacity using the design cross section of case 1.

Acknowledgment

We wish to express our gratitude to former students who contributed many experiments at Hokkaido Univ. and Hokkai Gakuen Univ.

References

[1] Standard Specification for Design and Construction of Concrete Structures, Japan Society of Civil Engineers, 1986
[2] Y. Takahashi and Y. Kakuta: Effect of Free Edge on Punching Strength of Reinforced Concrete Slabs, Transactions of JCI, pp.255-260, 1983
[3] Y. Kakuta, A. Ito, and Y. Fujita: An Experimental Study on Punching Shear Strength of Reinforced Concrete Slabs, Proceedings of JSCE, No.229, pp.105-115, 1974 (in Japanese)
[4] Vanderbilt, M.D.: Shear Strength of Continuous Plate, Proceedings of ACSE, ST 5, 1972
[5] Revision Material for the Standard Specification for Design and Construction of Concrete Structures, JSCE, Concrete Library, No.61, 1986 (in Japanese)
[6] CEB-FIP Model Code for Concrete Structures, CEB, 1978
[7] CEB-FIP Model Code 1990, CEB, 1990
[8] Building Code Requirements for Reinforced Concrete (ACI318M-89) and Commentary-ACI 318Rm-89, ACI, 1989
[9] Eurocode 2-1: Design of Concrete Structures - Part 1: General rules and buildings, 1991
[10] J. Niwa, et al: Re-evaluation of Equation for Shear Strength of Reinforced Concrete Beams without Web Reinforcement, Proceedings of JSCE, No.372, pp.167-176, 1986 (in Japanese)
[11] J. Niwa: Equation for Shear Strength of Reinforced Concrete Deep beams Based on FEM Analysis, Proceedings of JCI 2nd Colloquium on Shear Analysis of RC Structures, pp.119-128, 1983 (in Japanese)